The Meteoritical Society

Meteoritics & Planetary Science 48, Nr 4, 656–664 (2013)
doi: 10.1111/maps.12081

Moderate velocity oblique impact sliding: Production of shocked meteorite textures and palaeomagnetically important metallic spherules in planetary regoliths

David K. POTTER[1*] and Thomas J. AHRENS[†]

[1]Department of Physics, and Department of Earth and Atmospheric Sciences, University of Alberta, Edmonton, Canada
[†]Deceased. Formerly at the Seismological Laboratory 252-21, California Institute of Technology, Pasadena, California USA
[*]Corresponding author. E-mail: dkpotter@ualberta.ca

(Received 17 December 2011; revision accepted 17 December 2012)

Abstract–We detail the production of metallic spherules in laboratory oblique shock impact experiments, and their applicability (1) to textures in a partly shock-melted chondritic meteorite and (2) to the occurrence of palaeomagnetically important fine iron or iron alloy particles in the lunar regolith. Samples recovered from 29–44 GPa, 800 ns, experiments revealed melting and textures reminiscent of metallic spherules in the Yanzhuang H-chondrite, including "dumbbell" forms and other more complex morphologies. Our experiments demonstrate that metallic spherules can be produced via oblique impact sliding at lower velocities (1.85 km s^{-1}) than are generally assumed in previous work associated with bulk-shock melting, and that oblique impact sliding is a viable mechanism for producing spherules in shock-induced veins in moderately shocked meteorites. Significantly, our experiments also produced fine metallic (iron alloy) spherules within the theoretical narrow size range (a few tens of nanometers for slightly ellipsoidal particles) for stable single-domain (SSD) particles, which are the most important palaeomagnetically, since they can record lunar and planetary magnetic fields over geological time periods. The experiments also produced spherules consistent with superparamagnetic (SP) and multidomain (MD) particle sizes. The fine SSD and SP particles on the lunar surface are currently thought to have been formed predominantly by space weathering processes. Our experiments suggest that oblique shock impact sliding may be a further means of producing the SSD and SP iron or iron alloy particles observed in the lunar regolith, and which are likely to occur in the regoliths of Mercury and other planetary bodies.

INTRODUCTION

Shock loading of metallic samples can provide important insights into the formation of impact-induced textures, melt zones, and fine metallic particles in shocked meteorites and planetary regoliths. In this article, we use a novel experimental system, oblique interface configuration, to investigate shock-induced melting textures in two metals placed in contact. This configuration provides a convenient way of producing laboratory shock-induced textures, transformations, and chemical reactions in analog planetary samples subjected to shear stresses. We have previously reported its use in the study of a shock-induced chemical reaction whereby two single crystals of MgO (periclase) and Al_2O_3 (corundum) placed in contact produced $MgAl_2O_4$ spinel at the crystal–crystal interface (Potter and Ahrens 1994).

Metallic spherules are often found in shocked-chondritic meteorites (Begemann et al. 1992), lunar samples (See et al. 1986), and at terrestrial meteorite impact sites (Brett 1967; Blau et al. 1973; Kelly et al. 1974). In these cases, and occurrences of other types of impact melt spherules (Taylor and Brownlee 1991; Kyte and Bostwick 1995; Chadwick et al. 2001; Basu et al. 2003; Simonson 2003), the spherules are formed (or assumed to form) from massively shock-melted material. Whilst we believe that many impact spherules are indeed formed in this way, one of the main purposes of the present article is to demonstrate that, upon moderate velocity sliding, impact spherules can be

produced at much lower velocities than is usually assumed. Most previous studies have generally been associated with bulk-shock melting. We postulate that spherules might be produced in moderately shocked (<50 GPa) meteorites, particularly in shock-induced shear-melted veins. We previously produced localized melting along shear bands in shock experiments on single crystal Al_2O_3 (Potter and Ahrens 1994, Figs. 4b and 4c). We also discussed the possibility that our shock-generated $MgAl_2O_4$ spinel, at the interface of the two single crystals of MgO and Al_2O_3, was produced via localized shear melting at this interface as a result of grain boundary sliding frictional heating. Another study identified melt veins formed by rapid shear melting in the Martian meteorite Zagami (Langenhorst and Poirier 2000). Laboratory shock experiments have also demonstrated that shock veins due to shear melting can be produced in single crystal olivine (Langenhorst et al. 2002) similar to those observed in ordinary chondrites. We now look at oblique impact sliding in metals to gain insights into frictional shear melting at metal–metal interfaces and the possibility of producing metallic spherules as observed in the Yanzhuang H-chondrite (Begemann et al. 1992).

Returned lunar samples have also shown abundant fine metallic iron and iron alloy particles in the reducing conditions of the lunar surface regolith (Wänke et al. 1970). The lunar iron particles range from large multidomain (MD) particle sizes, where they may be up to several tens or hundreds of microns in diameter (Reed and Taylor 1974; Goldstein et al. 1975), down to stable single-domain (SSD) and superparamagnetic (SP) particles of a few tens of nanometres (Stephenson 1971; Butler and Banerjee 1975; Dunlop and Ozdemir 1997). There is a relatively higher proportion of the fine SSD and SP particles in the shocked-lunar breccias (Mason and Melson 1970; Dunlop et al. 1973; Dunlop and Ozdemir 1997). The SSD particles are particularly important since they are the best potential recorders of the natural remanent magnetization (NRM) in lunar rocks over geological time periods, and therefore hold key information regarding the palaeointensity of the ancient magnetic fields on the Moon, irrespective of whether those fields were due to a former internal dynamo or transient fields from impact processes. These palaeomagnetically important SSD iron and iron alloy particles theoretically occur over a very narrow size range (Butler and Banerjee [1975] predicted 15–60 nm if the particles are slightly prolate ellipsoids, and Bentley et al. [2009] have also modeled the SSD to SP transition size), and therefore it is important to know how these particles were formed and how abundant they are. Various mechanisms were initially postulated for the formation of the fine SSD and SP iron and iron alloy particles in the lunar regolith (Pearce et al. 1972; Housley et al. 1973; Blau and Goldstein 1975). For example, Housley et al.'s (1973) study involved shock in a reducing atmosphere. Subsequently, Rowan and Ahrens (1994) proposed shock-induced reduction of FeO from their experimental observations of shock loading mid-ocean ridge basalt (MORB) samples. They produced metallic spheres in a range of sizes up to a few tens of microns. Keller and McKay (1997), Pieters et al. (2000), Hapke (2001), and Sasaki et al. (2001) demonstrated that nanoparticles of iron can be formed through space weathering processes (such as vapor deposition from micrometeorite impacts).

Fine iron and iron alloy particles are also likely to be present in other planetary regoliths, such as that of Mercury. Mercury has experienced a greater impact rate than the Moon, and exhibits reflectance spectra and albedos that suggest material similar to some Apollo 16 breccias (Cintala 1992). The NRM of SSD iron and iron alloy particles could hold important clues concerning the magnetic history of the planet, with implications for its internal structure and evolution.

The observations of fine SSD and SP iron and iron alloy particles on the Moon, and the expected presence of such particles on Mercury and other planetary regoliths, provided the second main motivation for the present work. Specifically, we wanted to investigate whether moderate velocity oblique shock impact sliding of pre-existing metallic material (present in a planetary regolith and/or an iron meteorite impactor) can produce the fine-grained palaeomagnetically important SSD metallic iron or iron alloy, as well as the SP particles, irrespective of whether iron oxide reduction mechanisms and space weathering processes also operate.

As regards the abundance of SSD and SP particles it is worth noting that Bentley et al. (2009) have recently proposed an in situ magnetic susceptibility technique for estimating the quantity and size distribution of such fine-grained iron particles in planetary regoliths. Potter (2011) also proposes a rapid, nondestructive magnetic remanence technique to specifically detect the presence of the palaeomagnetically important SSD iron and iron alloy particles in lunar and other planetary regolith samples.

EXPERIMENTAL DETAILS

We first described the experimental set up and target assembly for oblique shock impact sliding in Potter and Ahrens (1994; see figs. 1 and 2 of that paper). In the present study a copper disk 1.25 cm in diameter and 0.048 cm thick was placed in a stainless steel capsule and inserted at an oblique angle θ into the target assembly housing (Fig. 1). A stainless steel flyer plate (1.59 cm in diameter and 0.25 cm thick) was

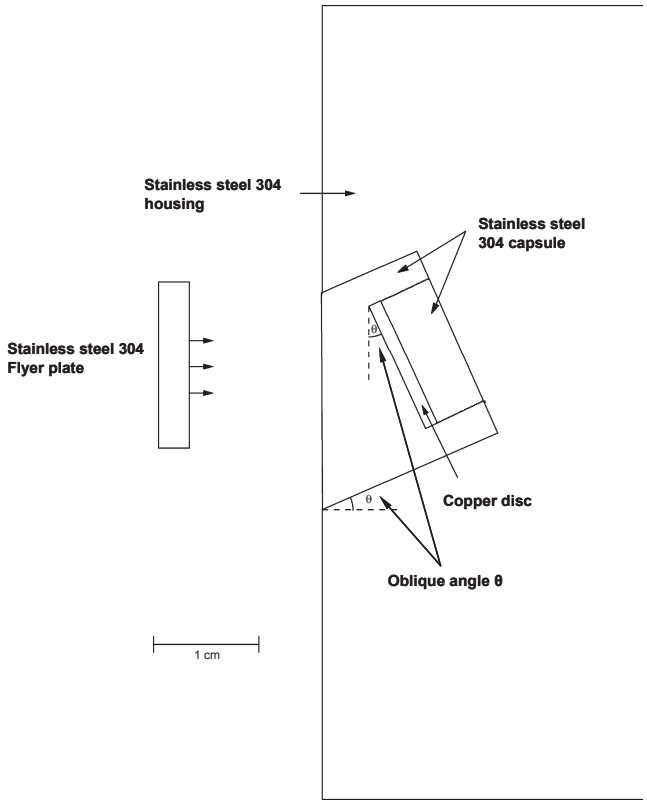

Fig. 1. Cross section of the experimental target assembly showing the oblique interface configuration.

accelerated to velocities between 1.33 and 1.87 km s^{-1} using the 20 mm gun at the Lindhurst Laboratory of Experimental Geophysics at Caltech and impacted against the capsule. A series of experiments at different oblique angles and projectile velocities were undertaken to determine whether melting and spherule formation can occur at the interface of the two metals. Copper provided a convenient matrix in which to capture and quantitatively analyze the range of iron alloy (stainless steel) spherule sizes and their morphology. We also partly chose to use copper as the matrix in these experiments as the contrast between the copper matrix and the stainless steel spherules on polished sections of the recovered samples was better than that for some initial tests we had performed with nickel and stainless steel and silicates and stainless steel. This allowed us to better characterize the steel spherules even though iron-nickel or iron-silicate oblique sliding combinations may be regarded as being more relevant to meteorites and planetary regoliths. We used stainless steel instead of pure iron partly because the 304 stainless steel comprised iron alloyed with nickel (8%) and chromium (18%) and both nickel and chromium are commonly associated with iron in lunar regolith samples, whilst nickel is associated with iron in the Yanzhuang H-chondrite meteorite. We realize, however, that chromium in meteoritic metal is low, usually <200 ppm, and that chromium in meteorites is generally in the silicates and oxides. Nevertheless, we considered the steel to be a reasonable analog for comparison with the iron and iron alloy particles in the lunar and meteorite natural samples. Furthermore, the melting temperature of pure iron is 1810 K whilst that for the stainless steel is very similar at 1800 K (Tennent 1971). Also, stainless steel was readily available and does not rust in the terrestrial atmosphere as we did not want our recovered polished samples to be influenced in any way by any potential thin oxide (rust) layers, particularly since iron and iron alloy particles on the lunar surface reside in nonoxidizing conditions.

The experimental conditions for a series of shots with different oblique angles and projectile velocities are given in Table 1. The given shock pressures (P_H) for copper and stainless steel are peak values for normal incidence impact, determined for the initial shock states via the impedance matching technique (Zeldovich and Raiser 1967) using the shock velocity (U_s) and particle velocity (u_p) data of Marsh (1980) for stainless steel 304 of density 7.890 g cm^{-3},

$$U_s \text{ (km s}^{-1}) = 4.58 + 1.49\ u_p \quad (1)$$

and for copper of density 8.924 g cm^{-3},

$$U_s \text{ (km s}^{-1}) = 3.91 + 1.51\ u_p \quad (2)$$

In reality, the shock pressures will be slightly lower for oblique impacts (Massey 1989). Using our calculated shock pressures the postshock continuum temperatures were then determined using data from McQueen et al. (1970). Again these were peak values for normal incidence impacts (the oblique values would again be slightly lower). Significantly, these theoretical continuum peak values are much lower than the melting temperatures of copper or iron from the copper-iron phase diagram (Massalski 1992).

RESULTS AND DISCUSSION

Optical microscopy, scanning electron microscopy (SEM), and energy dispersive X-ray analysis were performed on polished sections of the recovered samples. These analyses revealed melting at the rear copper-stainless steel interface (right-hand interface in Fig. 1) in shot numbers 912, 917, and 918 (Table 1). Note that melting only occurred at this interface, strongly suggesting that metal–metal sliding and frictional heating occurred. Since we observed melting, the temperatures must have exceeded the melting points of stainless steel

Table 1. Experimental conditions and calculated shock pressures and theoretical continuum temperatures.

Shot number	Sample	Oblique angle θ(degrees)	Projectile velocity (km s^{-1})	Shock pressure P_{H^*} (GPa)		Postshock temperature (K)		Recovered sample condition
				Stainless steel	Copper	Stainless steel	Copper	
883	Copper/ stainless steel	15	1.33	29.2	29.2	340	360	No melting. Hump feature.
912	Copper/ stainless steel	15	1.85	43.5	43.8	410	445	Interfacial waves, and vortices. Thin melt zone (40–50 μm thick) at rear metal–metal interface.
917	Copper/ stainless steel	25	1.85	43.5	43.8	410	445	Melt zone (120–300 μm thick) exhibiting stainless steel spherules at rear metal–metal interface.
918	Copper/ stainless steel	30	1.87	44.1	44.4	415	450	Some melt. No spherules.

*Initial shock states.

(1800 K) and copper (1356 K). These temperatures are significantly higher than the theoretically calculated postshock continuum temperatures (Table 1). The continuum temperatures, which are only relevant for uniform bulk shock heating, therefore do not adequately represent the temperatures generated at the metal–metal interface. Instead, it appears that melting temperatures were achieved at the metal–metal interface due to shear sliding frictional heating.

Of particular interest was the production of a range of liquid immiscibility textures within the melt zone at the rear copper–stainless steel interface from shot number 917 (oblique angle $\theta = 25°$ and the projectile velocity was 1.85 km s^{-1}). These revealed numerous stainless steel spherules within the copper matrix. Figure 2 shows an SEM image of some of these spherules within a 300 μm thick melt zone. Many of the laboratory–produced spherules exhibit partial coalescence or are in various states of merger. Of particular interest are characteristic "dumbbell" forms (bottom left of Fig. 2), where a narrow bridge of molten stainless steel connects two initial stainless steel spherules. Dumbbell forms are sometimes seen in other natural impact features such as splash-form tektites. Butler et al. (2011) have detailed numerical simulations of rotating fluid drops which can produce dumbbell shapes and other morphologies seen in such tektites (which tend to be 1–100 mm in size and therefore much larger than the spherules in the present study). In our laboratory experiments the dumbbell shapes are clearly the result of bridging between two initial spherules and do not appear to be due to the mechanism described by Butler et al. (2011). Evidence for this comes from the asymmetric dumbbell at the bottom left of Fig. 2 which exhibits bridging between two initial spherules of different size. We also see examples of bridging of three spherules as in the top right of Fig. 2, which would again appear to rule out the mechanism described by Butler et al. (2011) in our case.

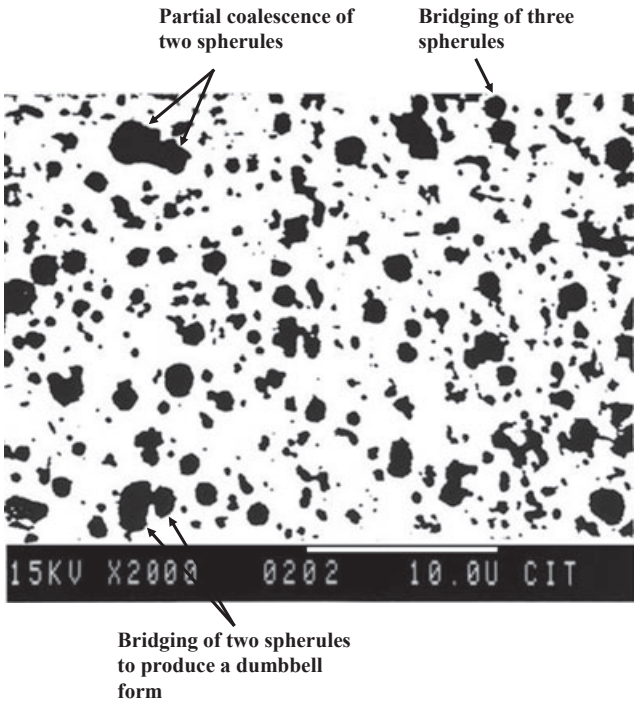

Fig. 2. SEM image of immiscibility melt textures produced at the rear copper–stainless steel interface from shot number 917 (oblique angle $\theta = 25°$ and a projectile velocity of 1.85 km s^{-1}). Stainless steel spherules (black) are shown within the copper matrix (white) in the melt zone. Scale bar = 10 μm. The contrast has been enhanced to show the outline morphology of the spherules, obscuring the rims that are seen in Fig. 5. Note the partial coalescence of some spherules, and the characteristic "dumbbell" shapes produced by the bridging of two spherules. Bridging of three spherules is also evident.

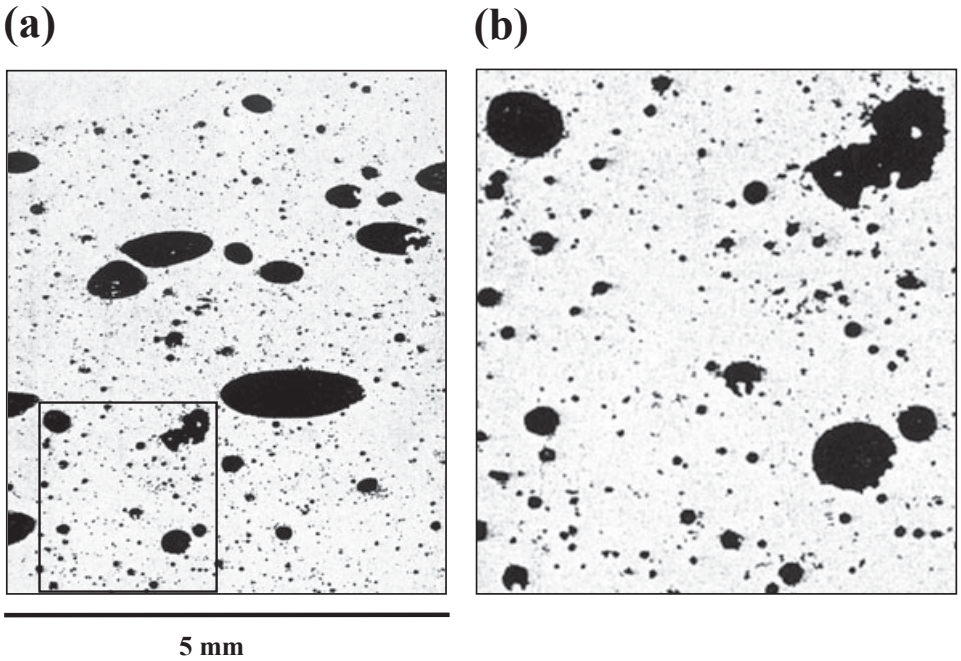

Fig. 3. a) Metallic spherules observed in a polished section of the shock-melted Yanzhuang H-chondrite meteorite (from fig. 1 of Begemann et al. 1992). The image is a negative of the original, for easy comparison with our laboratory-produced textures. The width of the field of view is 5 mm. b) Enlarged image of the area outlined in (a).

Meteorite Texture Comparisons

The experimentally produced spherules are reminiscent of metallic (FeNi-FeS) spherules seen in fig. 1 of Begemann et al. (1992) for the shock-melted Yanzhuang H-chondrite meteorite. The spherules produced in the Begemann et al. (1992) study are shown here in Figs. 3a and 3b, where we display the negative of the original images for easier comparison with our experimentally produced textures. Figures 4a and 4b show direct comparisons between features observed in the Yanzhuang H-chondrite and our laboratory-produced textures from shot number 917 (oblique angle $\theta = 25°$ and the projectile velocity was 1.85 km s^{-1}). Both the natural meteorite sample and the recovered experimental sample exhibit partially coalesced spherules with a slightly "dumbbell" looking form (highlighted in the rectangles in Figs. 4a and 4b). Other morphologies seen in both the natural meteorite and the laboratory-produced samples include "horseshoe" morphologies (highlighted by the circles in Figs. 4a and 4b). Furthermore, the meteorite and the laboratory-produced textures exhibit similar more complex structures. For example, the highlighted feature in the oval in Fig. 4b is a composite form resulting from two "teardrops" (each "teardrop" being the coalescence between two spherules of different size) combined with the bridging of the larger diameter portions of each teardrop. The morphology of the resulting composite looks quite similar to a grain in the natural Yanzhuang H-chondrite meteorite sample (rotate the laboratory-produced grain clockwise through 90° and compare it with a grain in the Yanzhuang H-chondrite meteorite sample, which is highlighted by the corresponding oval in Fig. 4a). However, there is a possibility that the natural grain might be the result of the coalescence of one (rather than two) larger initial spherule with two smaller spherules, rather than the result of a four spherule merger (two larger and two smaller) in the laboratory example.

The Yanzhuang meteorite is generally regarded as having been a heavily shocked meteorite, and so it is interesting to see similar features in our moderately shocked laboratory-recovered samples. Our laboratory-produced spherules (Figs. 2, 4, 5, and 6) exhibited a wide range of sizes, like the natural meteorite sample (Figs. 3a and 3b), however, the latter showed a broader range with spherules up to 2 mm in maximum dimension.

Relevance to Iron and Iron Alloy Particles in Lunar Samples

Production of Palaeomagnetically Important Stable Single-Domain Particles

The laboratory-produced stainless steel spherules ranged in size from a few microns down to a few tens of nanometres. Some were only about 20–30 nm in

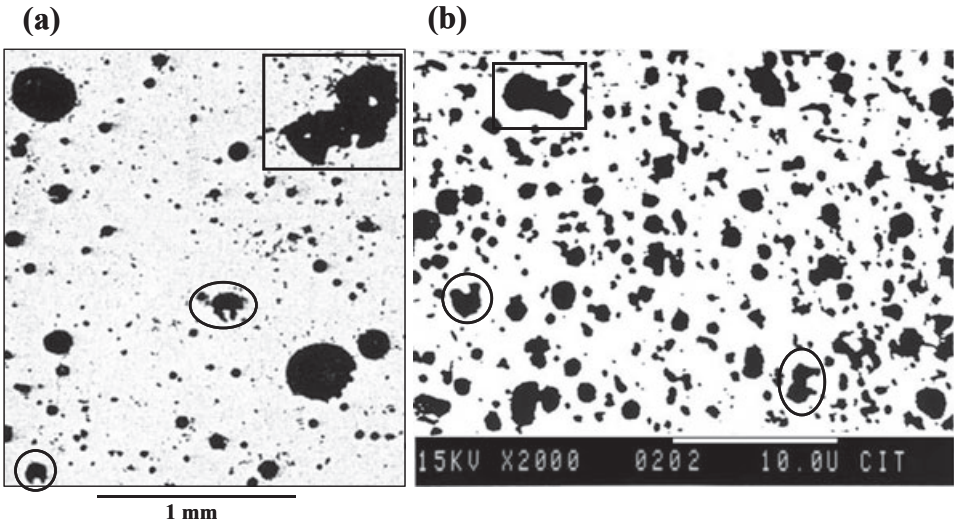

Fig. 4. Comparisons between the metallic spherules in (a) the Yanzhuang H-chondrite and (b) the laboratory shock-produced spherules from shot number 917. Partial coalescence of spherules (producing a slightly "dumbbell" looking shape) is seen in both the natural meteorite and laboratory samples (highlighted by the rectangles in (a) and (b)). Other features such as "horseshoe" morphologies are seen in both examples (highlighted by the circles in (a) and (b)). Similar looking more complex structures are also apparent in both the natural and laboratory samples. The oval in (b) highlights a composite merger of four spherules: two "teardrop" forms (each the merger of a larger spherule on the left with a smaller spherule on the right) whose larger diameter portions have merged. Compare this, by rotating it clockwise through 90°, with a grain in the natural Yanzhuang H-chondrite meteorite sample (highlighted by the oval in (a)).

diameter (200–300 Å). These nanoscale spherules are readily identified in the higher magnification SEM image (Fig. 5) from shot number 917. The range of experimentally produced spherules, had they been pure iron, are theoretically consistent with a range of magnetic domain states from larger MD particles to the narrow range of smaller palaeomagnetically more important SSD particles to the even finer SP particles (Butler and Banerjee 1975; Dunlop and Ozdemir 1997; Bentley et al. 2009). Butler and Banerjee (1975) theoretically predicted that there is no SSD size range for spherical metallic iron grains, but concluded that small slightly elongated iron grains (prolate ellipsoids having a ratio of maximum to minimum principal axes greater than 1.1) will have a SSD range if they are around 15–60 nm in size (150–600 Å). The small spherules in Fig. 5 are indeed slightly elongated (and not perfectly circular in cross section) and so the laboratory experiment does appear to be capable of producing SSD particles. Figures 6a and 6b show SEM images from another part of the rear copper-stainless steel interface from shot number 917, where the melt zone was around 120 μm in thickness. Here, there appears to have been more turbulent mixing, and many of the spherules (the nanoscale ones as well as the larger ones) exhibit even more pronounced anisotropic (elongated) shapes which is further strong evidence for the production of SSD particles. Thus, oblique shock impact sliding would appear to be a viable mechanism for producing palaeomagnetically important SSD particles, as well as SP particles, in the lunar regolith.

The size range of our experimentally produced spherules is also consistent with that of metallic iron particles seen in returned lunar regolith samples, such as the Apollo 14 breccias (table 17.1 of Dunlop and Ozdemir 1997). The morphologies and size range of the laboratory spherules are also similar to those observed for iron spheroids in a glass fragment from a lunar breccia (fig. 3.9 of Mason and Melson 1970).

Metallic Rims

Figure 5 shows that the spherules are surrounded by rims up to 1 μm thick, which are slightly darker than the copper matrix. Energy dispersive X-ray analysis showed that these rims contained between 1–4% iron. The copper-iron phase diagram (Massalski 1992) shows that molten nearly pure copper can dissolve this percentage of iron. Various types of rims have been observed in lunar grains, and may involve complex formation mechanisms. Keller and McKay (1997) classified four broad categories: amorphous, inclusion-rich, multiple, and vesicular. Inclusion-rich rims contain abundant nanometer-sized iron or iron alloy grains that are thought to result primarily from deposition of impact-generated vapors. While the rims in our experiments are

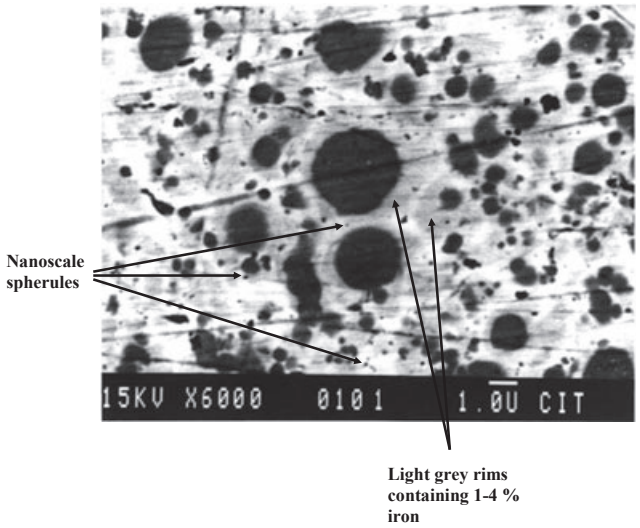

Fig. 5. Magnified image of stainless steel spherules (black) in copper matrix (white) produced at the rear copper–stainless steel interface from shot number 917. Scale bar = 1 μm. The image shows several nanoscale spherules (a few tens of nanometers in diameter), some of which are indicated by the arrows. Significantly these nanoscale spherules are consistent with the size range of palaeomagnetically important SSD particles. Such SSD particles theoretically only occur over a very narrow particle size range as described in the text, and are important recorders of planetary magnetic fields over geological periods. Our experiments demonstrate that oblique shock impact is one mechanism that can produce such particles. Some of the nanoscale spherules are of a size that would be consistent with them being SP particles (very slightly smaller than the SSD particles). The image also shows that there are larger spherules, which would be in the MD size range in terms of their magnetic properties. The spherules are surrounded by rims (light gray) containing 1–4% iron. The straight lines are scratches arising from the surface-polishing process.

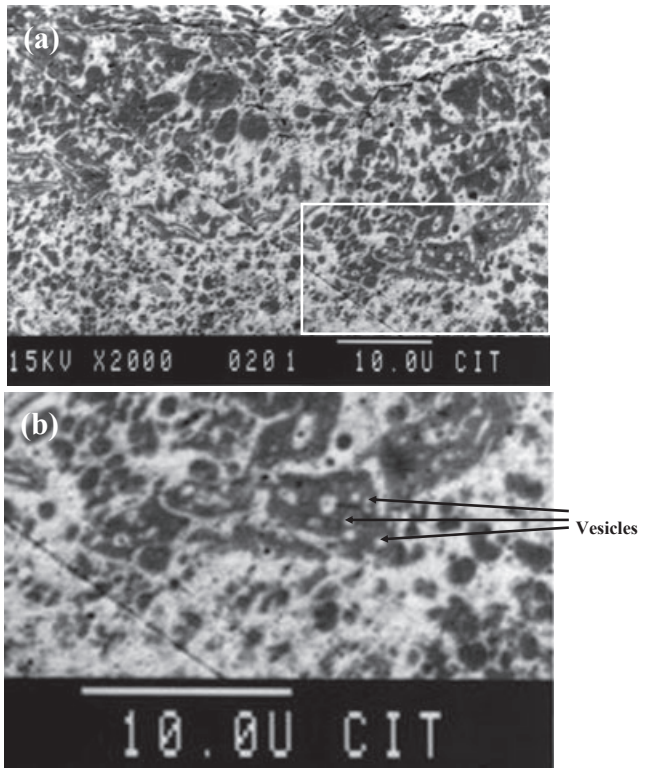

Fig. 6. a) SEM image from another region of the melt zone from shot number 917. Scale bar = 10 μm. The texture here indicates more turbulent mixing, with spherules exhibiting more extreme anisotropic shapes. Note also the presence of small vesicles within some spherules. b) Magnified view of the vesicles and spherules in the region highlighted by the rectangle at the bottom right of (a).

specifically related to the material combinations we have used, it is possible that some metallic rims in lunar grains may also be produced by the oblique shock impact mechanism described here.

Vesicles

Figures 6a and 6b also show that some of the spherules have very small vesicles (down to 250 nm) within them. The smallest vesicles are rare in terrestrial volcanics, but are found in lunar glass (Mason and Melson 1970, fig. 5.7; Keller and McKay 1997; Basu et al. 2002). Keller and McKay (1997) showed that many of these vesicles occur as vesicular rims in regolith grains, and are likely to have formed due to solar wind implanted gasses. Our experiments suggest that some vesicles in lunar regolith grains might be formed from the shock-induced processes described here.

CONCLUSIONS

Oblique shock impact sliding of metal–metal interfaces has generated melt layers, which exhibit a range of liquid immiscibility textures featuring metallic spherules. The laboratory-produced textures reveal a number of features that are very similar to those seen in the Yanzhuang H-chondrite meteorite (Begemann et al. 1992). The experimentally produced spherules exhibit various states of merger. Characteristic "dumbbell" shapes are shown in the present laboratory experiments to result from the bridging of two spherules. Crucially, our laboratory metallic spherules were produced by shear melting (the experiments strongly suggest this was due to frictional sliding heating) in moderately shocked samples, at lower impact velocities than those usually associated with bulk-shock melting. We therefore propose that oblique impact sliding may provide a mechanism for generating metallic spherules in shear-melted shock veins in moderately shocked meteorites.

Oblique shock impact sliding at moderate velocities also appears to be a viable complementary or alternative mechanism for producing fine iron or iron alloy particles in the lunar regolith and potentially other planetary regoliths. Significantly, the experiments suggest that both (1) palaeomagnetically important SSD particles, which theoretically occur over a very narrow particle size range (for prolate ellipsoidal particles), and (2) SP particles can be produced by this mechanism. On the lunar surface localized metal–metal sliding of pre-existing metal (in the regolith and/or in an iron meteorite impactor) through micro or macrometeorite impacts may have formed some of the SSD and SP material in a similar way. Much of this ultrafine-grained metallic material is currently attributed to space weathering processes (vapor deposition from micrometeorite impacts). Our experiments offer the possibility that some of this material may have formed by oblique impact sliding. Other experimentally produced features, such as rims around the spherules and nanoscale vesicles within the spherules, raise the possibility that some rims and vesicles in lunar grains may also be due to the shock-induced processes we describe here.

The observed shear melting due to frictional sliding heating adds support to our previous suggestion of possible melting at the crystal–crystal interface (producing a thin $MgAl_2O_4$ spinel layer) in similar oblique shock sliding experiments on single crystals of MgO and Al_2O_3 that were placed in contact (Potter and Ahrens 1994). We further demonstrated such melting along shock-induced shear bands in single crystal Al_2O_3 (Potter and Ahrens 1994), and shear melting has also been demonstrated experimentally in shocked single crystal olivine (Langenhorst et al. 2002). Nevertheless, we still cannot rule out the possibility that defect-enhanced solid state diffusion might account for the shock-produced spinel in our previous work.

Acknowledgments—Research supported by NASA. We thank Meteoritics & Planetary Science, © 1992 by the Meteoritical Society, for permission to reproduce fig. 1 of Begemann et al. (1992). We thank associate editor Randy Korotev and the two reviewers, Philippe Claeys and an anonymous reviewer, for their constructive comments which improved this manuscript.

Editorial Handling—Dr. Randy Korotev

REFERENCES

Basu A., Wentworth S. J., and McKay D. S. 2002. Heterogeneous agglutinitic glass and the fusion of the finest fraction (F^3) model. *Meteoritics & Planetary Science* 37:1835–1842.

Basu A. R., Petaev M. I., Poreda R. J., Jacobsen S. B., and Becker L. 2003. Chondritic meteorite fragments associated with the Permian-Triassic boundary in Antarctica. *Science* 302:1388–1392.

Begemann F., Palme H., Spettel B., and Weber H. W. 1992. On the thermal history of heavily shocked Yanzhuang H-chondrite. *Meteoritics* 27:174–178.

Bentley M. S., Ball A. J., Potter D. K., Wright I. P., and Zarnecki J. C. 2009. In-situ multi-frequency measurements of magnetic susceptibility as an indicator of planetary regolith maturity. *Planetary and Space Science* 57:1491–1499.

Blau P. J. and Goldstein J. I. 1975. Investigation and simulation of metallic spherules from lunar soils. *Geochimica et Cosmochimica Acta* 39(3):305–324.

Blau P. J., Axon H. J., and Goldstein J. I. 1973. Investigation of the Canyon Diablo metallic spheroids and their relationship to the breakup of the Canyon Diablo meteorite. *Journal of Geophysical Research* 78:363–374.

Brett R. 1967. Metallic spherules in impactite and tektite glasses. *American Mineralogist* 52:721–733.

Butler R. F. and Banerjee S. K. 1975. Single-domain grain size limits for metallic iron. *Journal of Geophysical Research* 80:252–259.

Butler S. L., Stauffer G., Sinha A., Lilly A., and Spiteri R. J. 2011. The shape distribution of splash-form tektites predicted by numerical simulations of rotating fluid drops. *Journal of Fluid Mechanics* 667:358–368.

Chadwick B., Claeys P., and Simonson B. M. 2001. New evidence for a large Palaeoproterozoic impact: Spherules in a dolomite layer in the Ketilidian orogen, South Greenland. *Journal of the Geological Society of London* 158: 331–340.

Cintala M. J. 1992. Impact-induced thermal effects in the lunar and Mercurian regoliths. *Journal of Geophysical Research - Planets* 97:947–973.

Dunlop D. J. and Ozdemir O. 1997. Rock magnetism fundamentals and frontiers. Cambridge, UK: Cambridge University Press. 573 p.

Dunlop D. J., Gose W. A., Pearce G. W., and Strangway D. W. 1973. Magnetic properties and granulometry of metallic iron in lunar breccia 14313. Proceedings, 4th Lunar Science Conference. pp. 2977–2990.

Goldstein J. I., Axon H. J., and Agrell S. O. 1975. Grape cluster, metal particle 63344,1. *Earth and Planetary Science Letters* 28:217–224.

Hapke B. 2001. Space weathering from Mercury to the asteroid belt. *Journal of Geophysical Research* 106 (E5): 10,039–10,073.

Housley R. M., Grant R. W., and Patton N. E. 1973. Origin and characteristics of excess Fe metal in lunar glass welded aggregates. Proceedings, 4th Lunar Science Conference. pp. 2737–2749.

Keller L. P. and McKay D. S. 1997. The nature and origin of rims on lunar soil grains. *Geochimica et Cosmochimica Acta* 61:2332–2341.

Kelly W. R., Holdsworth E., and Moore C. B. 1974. The chemical composition of metallic spheroids and metallic particles within impactites from Barringer Meteor Crater, Arizona. *Geochimica et Cosmochimica Acta* 38:533–543.

Kyte F. T. and Bostwick J. A. 1995. Magnesioferrite spinel in Cretaceous/Tertiary boundary sediments of the Pacific basin: Remnants of hot, early ejecta from the Chicxulub impact? *Earth and Planetary Science Letters* 132:113–127.

Langenhorst F. and Poirier J. P. 2000. Anatomy of black veins in Zagami: Clues to the formation of high-pressure phases. *Earth and Planetary Science Letters* 184:37–55.

Langenhorst F., Poirier J. P., Deutsch A., and Hornemann U. 2002. Experimental approach to generate shock veins in single crystal olivine by shear melting. *Meteoritics & Planetary Science* 37:1541–1553.

Marsh S. P., ed. 1980. LASL shock hugoniot data. Berkeley, CA: University of California Press. 658 p.

Mason B. and Melson W. G. 1970. *The lunar rocks*. New York: Wiley-Interscience. 179 p.

Massalski T. B., ed. 1992. *Binary alloy phase diagrams, 2nd edition, volume 2, copper-iron*. Novelty, OH: ASM International. p. 1409.

Massey B. S. 1989. *Mechanics of fluids*, 6th ed. London: Chapman and Hall. 599 p.

McQueen R. G., Marsh S. P., Taylor J. W., Fritz J. N., and Carter W. J. 1970. The equation of state of solids from shock wave studies. In *High velocity impact phenomena*, edited by Kinslow R. New York: Academic Press. pp. 293–417.

Pearce G. W., Williams R. J., and McKay D. S. 1972. The magnetic properties and morphology of metallic iron produced by subsolidus reduction of synthetic Apollo 11 composition glasses. *Earth and Planetary Science Letters* 17:95–104.

Pieters C. M., Taylor L. A., Noble S. K., Keller L. P., Hapke B., Morris R. V., Allen C. C., McKay D. S., and Wentworth S. 2000. Space weathering on airless bodies: Resolving a mystery with lunar samples. *Meteoritics & Planetary Science* 35:1101–1107.

Potter D. K. 2011. Novel magnetic techniques for rapidly detecting palaeomagnetically important single-domain iron particles and obtaining directional palaeomagnetic data from "unoriented" lunar rock samples. *Canadian Aeronautics and Space Journal* 57(1):12–23.

Potter D. K. and Ahrens T. J. 1994. Shock induced formation of $MgAl_2O_4$ spinel from oxides. *Geophysical Research Letters* 21:721–724.

Reed S. J. B. and Taylor S. R. 1974. Meteoritic metal in Apollo 16 samples. *Meteoritics* 9:23–34.

Rowan L. R. and Ahrens T. J. 1994. Observations of impact-induced molten metal-silicate partitioning. *Earth and Planetary Science Letters* 122:71–88.

Sasaki S., Nakamura K., Hamabe Y., Kurahashi E., and Hiroi T. 2001. Production of iron nanoparticles by laser irradiation in a simulation of lunar-like space weathering. *Nature* 410:555–557.

See T. H., Horz F., and Morris R. V. 1986. Apollo 16 impact-melt splashes—Petrography and major-element composition. *Journal of Geophysical Research* 91:E3–E20.

Simonson B. M. 2003. Petrographic criteria for recognizing certain types of impact spherules in well-preserved Precambrian successions. *Astrobiology* 3:49–65.

Stephenson A. 1971. Single domain grain distributions. II. The distribution of single domain iron grains in Apollo 11 lunar dust. *Physics of the Earth and Planetary Interiors* 4:361–369.

Taylor S. and Brownlee D. E. 1991. Cosmic spherules in the geologic record. *Meteoritics* 26:203–211.

Tennent R. M. 1971. *Science data book*. Harlow, UK: Oliver and Boyd. 104 p.

Wänke H., Wlotzka F., Jagoutz E., and Begemann F. 1970. Composition and structure of metallic iron particles in lunar "fines." Proceedings of the Apollo 11 Lunar Science Conference. pp. 931–936.

Zeldovich Y. and Raiser Y. P. 1967. *Physics of shock waves and high temperature hydrodynamic phenomena*, vol. 2. New York: Academic Press. 916 p.